1

Nanotechnology and Nanoparticles

CHAPTER MENU

Nanoparticles and Their Functions, 1
Classification of NPs, 2
Carbon-Based NPs, 2
Metal Nanoparticles, 2
Ceramic NPs, 3
Semiconductor NPs, 3
Polymeric NPs, 3
NPs Based on Lipids, 4
Synthesis of Nanoparticles, 4
Top-Down Synthesis, 4
Bottom-Up Synthesis, 5
NPs and Characterization, 6
Morphological Characterization, 6
Structural Characteristics, 7
Particle Size and Surface Area Characterization, 8
Optical Characterizations, 8
Physicochemical Properties of NPs, 9
Mechanical and Optical Properties, 9
Magnetic Properties, 9
Mechanical Properties, 10
Thermal Properties, 10
Functions of NPs, 10
Drugs and Medications, 11
Materials and Manufacturing, 11
Environment, 12
Electronics, 12
Energy Harvesting, 12
References, 13

COPYRIGHTED MATERIAL

1.1 Nanoparticles and Their Functions

Since the past century, nanotechnology has been an advanced research area. RP Feynman coined the term 'nanotechnology' during his famous speech [1]. Nanotechnology developed different types of nanoscale materials. A limited class of one-dimensional materials <100 nm [2] are nanoparticles (NPs). Depending on the form [3], such materials may be 0D, 1D, 2D, or 3D. The importance of these materials showed that the physicochemical

Nano-Technological Intervention in Agricultural Productivity, First Edition.
Javid A. Parray, Mohammad Yaseen Mir and Nowsheen Shameem.
© 2021 John Wiley & Sons Ltd. Published 2021 by John Wiley & Sons Ltd.

properties of a substance, e.g. the optical properties, can be influenced by size. The red wine, yellowish-grey, black, and deep green are the distinctive colours of the 20 nm gold (Au), platinum (Pt), silver (Ag), and palladium (Pd) NPs. These NPs exhibit distinctive colours and properties of various sizes and shapes that can be used in bioimaging applications. [4]. Owing to differences in aspect ratio, nanoshell thickness, and Au concentration, the solution's colour varies. Changing each of the elements mentioned above affects the absorption characteristics of the NPs and is therefore observed in different absorption colours. Usually, NPs consist of three layers: (i) a layer-functionalized surface with several tiny molecules, metal ions, surfactants, and polymers; (ii) a shell layer – a chemically separate core substance; and (iii) a centre – an integral part of the NP and typically refers to the NP itself [5]. Researchers gained immense interest in multidisciplinary fields because of these exceptional features. NPs may be used for the delivery of drugs [6], chemical and biological sensing [7], gas sensing [8], CO_2 capture [9], and related uses [10].

1.2 Classification of NPs

NPs are commonly classified according to morphology, size, and chemical properties in different classes. NPs are classified according to physical and chemical characteristics as follows.

1.2.1 Carbon-Based NPs

Two key NP groups based on carbon are fullerenes and carbon nanotubes (CNTs). Fullerenes contain globular hollow cage nanomaterials, similar to allotropic carbon forms. Their electrical conductivity, high power, structure, electron affinity, and flexibility have created considerable commercial interest [11]. Pentagonal and hexagonal C- units were arranged in these materials while each carbon was hybridized. The illustration in Figure 1.1 shows some of the well-known 7.114 and 7.648 nm C_{60} and C_{70} fullerenes. The long, tubular CNTs have a diameter of 1–2 nm [12]. This can be predicted as metallic or semiconducting based on their telicity diameter [13]. Single, double, or multiple walls may be rolling sheets labelled single-walled nanotubes (SWNTs), double-walled nanotubes (DWNTs), or multi-walled carbon nanotubes (MWNTs), respectively. They are commonly synthesized by carbon precursor deposition, particularly atomic carbons, which are vaporized by a laser or electric arc through metal particles. Recently, they have been synthesized using the chemical vapour deposition (CVD) technique [14]. Because of their specific physical, chemical, and mechanical characteristics, these materials are widely used in industrial applications, not only in pristine form but also in nanocomposites such as fillers [15], active gas adsorbents for the remediation of the environment [16], and, in general, for various inorganic and organic catalysts [17].

1.2.2 Metal Nanoparticles

Metal NPs comprise metal-made precursors. Because of the well-localized surface plasma resonance (LSPR) characteristics, such NPs have distinct optoelectronic properties. In the visible region of the solar electromagnetic spectrum, the NPs of alkali and noble metals

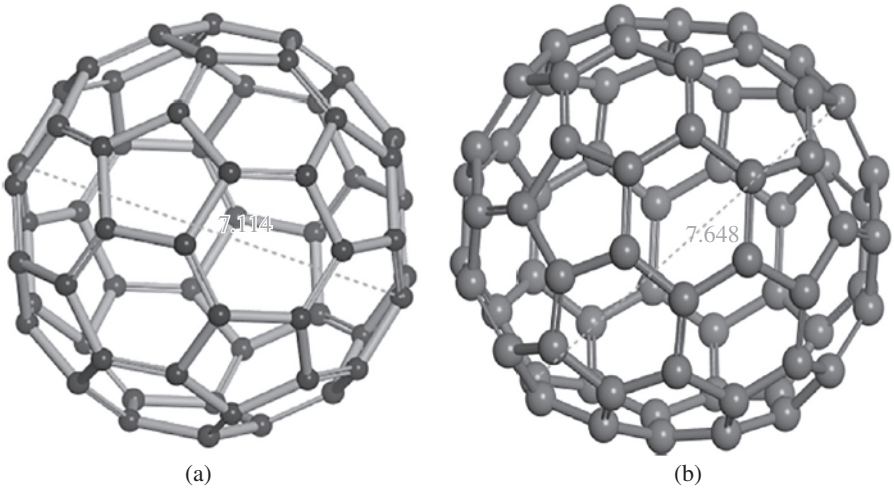

Figure 1.1 Description of fullerenes or buck balls (a) C_{60} and (b) C_{70}. Source: From Khan et al. [2]. © 2017, Elsevier.

such as Cu, Ag, and Au have broadband absorption. In today's cutting-edge materials, the facet, size, and shape-controlled synthesis of metal NPs are critical [4]. Metal NPs are finding applications in many research fields because of their advanced optical properties. The coating of gold NPs is widely used to enhance electronic streaming for scanning electron microscopy (SEM) sampling, thus helping to accomplish good SEM images.

1.2.3 Ceramic NPs

NPs from ceramics are inorganic non-metallic solids synthesized by heat and cooling. They are used in amorphous, polycrystalline, solid, porous, or hollow [18] forms. Because of their use in catalysis, photocatalysis, colour photodegradation, and imaging, these NPs offer substantial interest from researchers [19].

1.2.4 Semiconductor NPs

Semiconductor materials have properties between metals and non-metals, and because of this property, they find different applications in the literature [20]. Semiconductor NPs have large band gaps, demonstrating significant modifications to their properties with band gap tuning. Items of great significance also include photocatalysis, photo-optics, and electronic devices [21]. Because of their appropriate band gap and band edge positions, the range of semiconductor NPs is considered exceptionally efficient in water splitting applications [22].

1.2.5 Polymeric NPs

These substances are used for a wide range of commercial applications, such as fillers [15], effective adsorbents of environmental remedial gases [16], and as a support medium for various inorganic and organic calculators because they give specific physical, chemical, and mechanical characteristics [23].

1.2.6 NPs Based on Lipids

In many biomedical applications, they are used, and they contain lipid molecules. Usually, the lipid NP is spherical, 10–1000 nm in diameter. Similar to polymeric NPs, lipid NPs have a solid lipid core and lipophilic molecules within the matrix. The external centre of these NPs has been stabilized by surfactants or emulsifiers [24]. Lipid nanotechnology [25] is a specific field that focuses on the design and synthesis of lipid NPs for various applications, such as drug carriers and delivery [26] and the release of RNA cancer therapy [27].

1.3 Synthesis of Nanoparticles

Various techniques can be used for the synthesis of NPs. Nevertheless, these approaches are generally divided into two main categories, i.e. (i) top-down approach and (ii) bottom-up approach [28, 29] (Figure 1.2). These methods are further divided into different subclasses based on process, reaction state, and adopted protocols.

1.3.1 Top-Down Synthesis

The larger molecules are disintegrated into smaller units by a destructive process, and these units are transformed into useful NPs, for example, grinding/milling, CVDs, physical vapour deposition, etc. [29]. This approach is generally used to synthesize NPs from coconut shells (CSs). The milling method is used, whereby raw CS powders were finely milled using ceramic balls and a well-known planetary mill at different time intervals. Via other characterization techniques, the influence of the milling period on the overall size of the NPs is shown.

Furthermore, as time increases, the size of the NP crystallite (Scherrer equation) decreases. In this process, it was also found that the brownish colour faded away with the increment of each hour because of the reduced size of the NPs [30]. Various

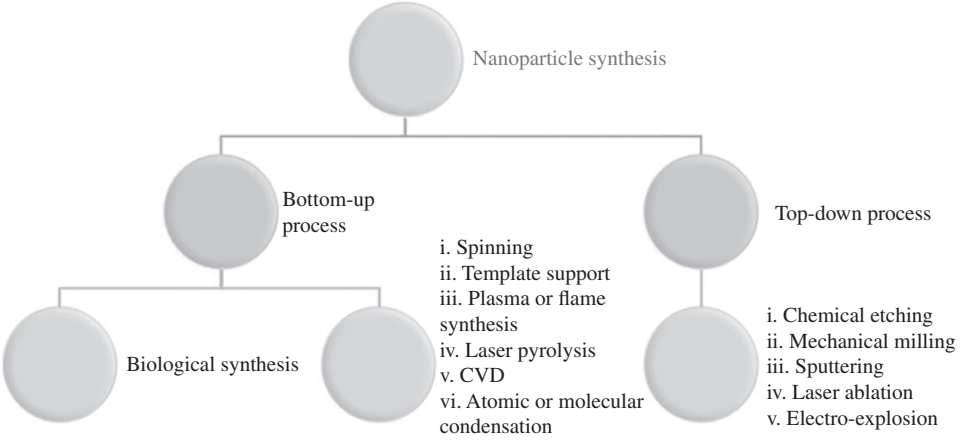

Figure 1.2 The synthetic models of NPs: top-down and bottom-up approach. Source: Modified from Iravani [29].

characterization techniques demonstrated the effect of milling time on the overall size of the NPs. The synthesis of spherical magnetite NPs from natural iron oxide (Fe_2O_3) ore was shown in the presence of organic oleic acid by a destructive top-down method with a particle size ranging from 20 to 50 nm [31]. To synthesize spherical particles of colloidal carbon using a control scale, a primary top-down route was used. The synthesis technique was based on the continuous chemical adsorption of polyoxometalates on the carbon interfacial surface. Adsorption has transformed black carbon aggregates into relatively smaller spherical particles with a high dispersion capacity and a narrow distribution of size [32]. Microstructures have found that the quantity of carbon particles is lower during the sonication period. Combined grinding and top-down sonication techniques synthesized a sequence of transition metal dichalcogenide nanodots (TMD-NDs) from their crystallites. Every TMD-ND with a size of less than 10 nm shows excellent dispersion and is demonstrated by the narrow distribution of the measure [33]. Highly photoactive Co_3O_4 NPs have recently been produced by top-down laser fragmentation, i.e. a top-down process with an average size of 5.8 ± 1.1 nm. Powerful laser irradiations produce well-uniformed NPs with adequate oxygen vacancy [34].

1.3.2 Bottom-Up Synthesis

This reverse approach is used to synthesize NPs from relatively more straightforward substances and is also called an approach to building up. Examples include sedimentation and reduction techniques. It encompasses sun-freezing, green synthesis, spinning, and biochemical synthesis [29]. Mogilevsky et al. [35] used this technique to synthesize TiO_2 anatase NPs to the graphene domains. Alizarin and titanium isopropoxide precursors have been used to synthesize the photoactive composite for methylene blue photocatalytic degradation. The X-ray diffraction (XRD) framework has verified the anatase form [35]. Well-uniform spherical shaped Au nanospheres have been synthesized with monocrystalline using top-down laser irradiation technique [36, 37]. Recently, the solvent exchange method has been used to deliver medical cancer drugs to achieve limited-size low-density lipoprotein (LDL) NPs. The standard approach followed by growth, i.e. up process, is nucleation in this technique. The LDL NPs were obtained without phospholipid use and had high hydrophobicity, which is a prerequisite for drug delivery implementation. [38]. The monodispersed spherical bismuth (Bi) NPs, with top-down and bottom-up approaches, are synthesized with excellent colloidal properties [39]. In bottom-up ethylene glycol, bismuth acetate was melted, although bismuth was converted into a molten state in the top-down process. In boiled diethylene glycol, the molten drop then has been emulsified for NPs. Both methods generated different NPs in size from 100 to 500 nm [39] (Figure 1.3a,b). Green and biogenic bottom-up processing is cost-effective and environmentally sustainable, where biological processes, such as using plant extracts, achieve the synthesis of NPs. For the synthesis of NPs, bacteria, yeast, fungi, *Aloe vera*, tamarind, and even human cells are used. Au-NPs were synthesized from wheat biomass and oat [40] and used as a reduction agent by microorganisms and plant extracts [41, 42]. Figure 1.3 demonstrated the bottom-up (Figure 1.3a) method: decomposing a molecular precursor into simple metal atoms, which transform into colloids and the top-down (Figure 1.3b) method.

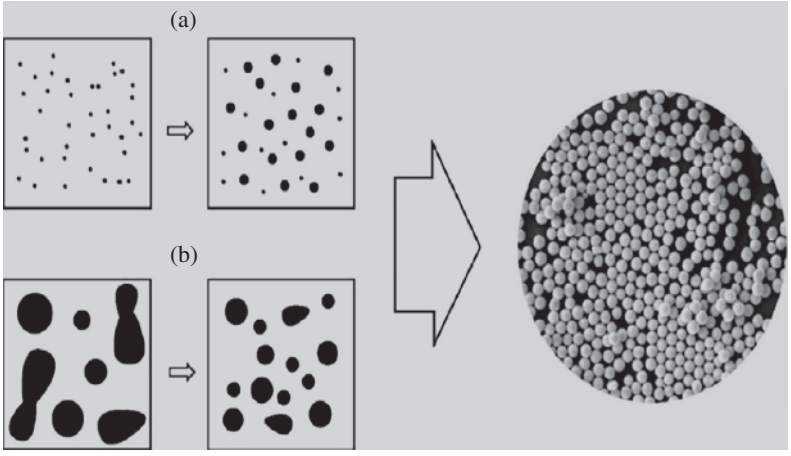

Figure 1.3 Illustration of synthesis of nanoparticles: (a) top-down method and (b) bottom-up method. Source: From Wang and Xia [39]. © 2004, American Chemical Society.

1.4 NPs and Characterization

For the analysis of other physicochemical properties of NPs, different methods of characterization have been used, such as XRD, X-ray photoelectron spectroscopy (XPS), infrared (IR), SEM, transmission electron microscopy (TEM), and Brunauer–Emmett–Teller (BET). Advanced methods are applied for the analysis of the particles.

1.4.1 Morphological Characterization

The morphological characteristics of NPs are still of great importance as morphology still affects most of the NP properties. Various characterization techniques exist for morphological research, but microscopic methods exist, such as polarized optical microscopy (POM), SEM, and TEM.

1.4.1.1 SEM Technique

The SEM technique is based on the electron scanning principle and provides all the nanoscale NP data available. This technique is used to study the morphology of their nanomaterials and the dispersion of NPs in the bulk or matrix. This technique [15] showed the distribution of SWNTs in polymer matrix poly(butylene) terephthalate (PBT) and nylon-6. The morphological characteristics of ZnO-modified metal–organic frameworks (MOFs) were studied using the SEM technique, which indicates the dispersion of ZnO-NPs and MOFs' morphologies under different reaction conditions [43].

1.4.1.2 TEM Technique

It is based on the electron transfer principle, so that it can provide descriptions of the bulk content from very low to greater magnification. In addition, it is commonly used for the analysis of different morphologies of the Au-NPs [44]. TEM also provides essential information about two- or more layer materials; the quadruple hollow shell structure of Co_3O_4

NPs is observed by TEM, for instance. In Li-ion batteries such as the anode, these NPs have proven themselves to be exceptionally efficient. The porous multi-shell structure induces shorter Li^+ diffusion path lengths with ample annulled space for buffer volume expansion, good cycling efficiency, higher speed capacity, and essential capacity [45].

1.4.2 Structural Characteristics

The structural characteristics of the structure and function of the bonding materials are of primary importance for studying. It gives details about the bulk properties of the subject material. XRD, energy-dispersive X-ray (EDX) spectroscopy, XPS, IR, Raman spectroscopy, BET, and Zieta size analyser are the techniques used to study the structural properties of NPs.

1.4.2.1 XRD

One of the essential characterization techniques is to reveal the structural properties of NPs. The crystalline phase of NPs is provided with sufficient data. It also provides a rough image of the particle size through the Debye–Scherrer [8] formula. In the identification of single and multiphase NP [46] schemes, this approach worked well. However, in smaller NPs with a size smaller than hundreds of atoms, the acquisition and accurate measurement of structural and other parameters may be difficult. Besides, the XRD diffractogram can be affected by NPs with different interatomic lengths having more amorphous characteristics. To obtain accurate data, the diffractograms of bimetallic NPs must be contrasted with those of the corresponding monometallic NPs and their physical mixtures in this case. The best way to make a substantial difference is to measure the simulated bimetallic NP structural model with the spectra of XRD [47] observed.

1.4.2.2 Energy-Dispersive X-ray (EDX)

To understand the elementary composition with a rough idea of per cent weight, a usually fixed field emission scanning electron microscopy (FE-SEM) or TEM system is commonly used. The electron beam centred on a single NP through SEM or TEM through the software functions to obtain the insight knowledge under observation from the NP. NP consists of constituent elements and, by irradiating electron beams, each of these releases X-ray energy characteristics. The real X-ray intensity is directly proportional to the explicit part of the particle's concentration. Researchers in preparatory materials commonly use this technique to help SEM and other processes to validate their components [48]. The elemental composition of ultra–sonochemically synthesized $BiVO_4$ NPs in pseudo-flower form [49] was calculated using the EDX technique. Similarly, a similar approach was used to perform the indispensable confirmation and graphene impregnation of Ln_2O_3/graphene heterostructure NPs, which showed C, Ln, and O as contributing elements synthesized by the traditional hydrothermal method [50].

1.4.2.3 XPS

It is a surface-sensitive tool and can be used to consider the overall composition and the compositional variance with in-depth profiling studies. XPS is based on the basic principles of spectroscopy. The typical XPS spectrum consists of the number of electrons on the Y-axis

plot versus the *X*-axis electrons' binding energy (eV). Each element has its fingerprint value for energy binding and thus gives a particular set of XPS peaks. Corresponding peaks, such as 1s, 2s, 2p, and 3s, come from the electronic configuration [51]. To research the dispersion of Boron NPs (10 nm size) during functionalization with polyethylene glycol (PEG), a depth profile analysis was given with Ar^+ ions at 1.4 keV and 20 nm. It has been shown that the concentration of NPs increases from 2% to 5% with depth. This offered strong evidence that within the bulk of functionalized PEG, boron NPs are effectively dissolved [52]. In a related analysis, core–shell Au/Ag showed similar behaviour through XPS scope profiling [53].

1.4.2.4 FT-IR and Raman Spectroscopies

The vibration characterization of NPs is typically studied by FT-IR and Raman spectroscopies. These techniques are the most evolved and feasible compared to other simple analytical methods. The critical range for NPs is the fingerprint region, which provides the details for the material signature. In one sample, Pt-NP (1.7 nm) functionalization and its interaction with the alumina substrate were analysed using FT-IR and XPS techniques. FT-IR confirms the functionality as it showed signature vibrational peaks of carboxylated C–O 2033 cm^{-1}, in addition to a broader O–H peak of 3280 cm^{-1}, respectively [54, 55]. Because of its signal-enhancing capability via SPR phenomenon, recently improved surface-enhanced Raman spectroscopy (SERS) is emerging as a vibrational conforming tool [56, 57].

1.4.3 Particle Size and Surface Area Characterization

Various techniques can calculate the size and surface area of the NPs. These include dispersing SEM, TEM, XRD, AFM, and dynamic light scattering (DLS). It is possible to increase the particle size of SEM, TEM, XRD, and AFM, but the zeta theoretical analyser/DLS should be used to find the NP size at a weak stage. In one study, DLS was used to analyse silica NP size differences while consuming serum proteins. With the acquisition of the protein layer, the findings showed that the size increased. However, in the case of aggregation and hydrophilicity, DLS might prove incapable of accurate measurement, so in that case, we should focus on the high-resolution technique of differential centrifugal sedimentation [58–60].

1.4.4 Optical Characterizations

Optical characteristics are of great concern in photocatalytic applications, and photochemists have therefore gathered a good understanding of this approach to reveal their photochemical processes [61, 62]. These are based on the common law of Beer–Lambert and the basic principles of light [63]. These methods include information about the absorption, reflectance, luminescence, and phosphorescence of nanomaterials. Metallic and semiconductor NPs have various colours and are thus ideally suited for photo-related applications. To understand each application's primary mechanism, it is often essential to see the importance of absorption and reflectance of these materials. UV–vis and photoluminescence are the most common optical devices used to study the optical properties of NP materials (PL, Null Ellipsometer). The Diffuse reflectance spectroscopy (DRS) UV/vis

is a fully designed optical absorption, transmission, and reflection measurement unit. The first two are extra, while DRS is mostly a unique technique for the samples sold. It is imperative to use the method for measuring NP band gaps as well as other NPs. MMT, $LaFeO_3$, and $LaFeO_3$/MMT nanocomposite synthesis and differences in their absorption of electromagnetic radiation by UV–vis DRS to identify their optical characteristics were studied [64]. In the case of nanocomposites, a significant red shift was observed compared to pristine MMT and $LaFeO_3$ NPs. Instead of a broad absorption band from 400 to 620 nm, $LaFeO_3$ and $LaFeO_3$/MMT revealed a reduction in their band gap. These NPs are significant for photocatalysis by solar light [64]. To investigate the optical properties of photoactive NPs and other nanomaterials and UV, PL considers useful technologies. This technique gives further information on the absorption or emission potential of the materials and their effects on the picture's overall excitement period. It thus provides valuable details about the charging hybridization and half-life of the exciting material on their conducting bands for all photo- and image applications.

1.5 Physicochemical Properties of NPs

Different physicochemical features such as the large surface are discussed; as previously mentioned, mechanically robust, optically active, and chemically reactive NPs are unique and ideal for multiple uses. Some of its essential properties are discussed in the following.

1.5.1 Mechanical and Optical Properties

There is greater interdependence between the optical and electronic properties of NPs. The noble metal NPs, for example, display full UV–visible extinction bands not available on the bulk metal spectrum and have visual properties that are dependent on size. When the conduction electrons' mutual excitation is aroused, this band of enthusiasm results in a continuous photon occurrence, known as the LSPR. LSPR excitation results in wavelength selection absorption with a large Ray light scattering coefficient of molar excitation resonance with an efficiency equal to that of 10 fluorophores and enhanced local electromagnetic fields near the surface of NPs, which strengthened spectroscopy. It is well known that the absorption spectrum of the LSPR spectrum relies on the size, shape, and interparticle spacing of the NPs, as well as its dielectric and local characteristics, such as substrates, solvents, and adsorbents [65]. The rusty colours seen in the door/windows of blemished glass are gold colloidal NPs responsibility, while Ag NPs are usually yellow. The free electrons on the surface are easily transportable via the nanomaterial in these NPs (d electrons in Ag and gold). For Ag and gold, the mean open path is 50 nm, more than the size of these materials in NPs. Thus, no scattering is required from the bulk after weak interaction. Instead, in these NPs, they set up standing resonance conditions responsible for LSPR [66, 67].

1.5.2 Magnetic Properties

For researchers from various disciplines, including heterogeneous and homogeneous catalysis, biomedicine, magnetic fluids, data storage for magnetic resonance imaging (MRI), and

environmental remediation such as water decontamination, magnetic NPs are of considerable interest. The literature indicates that NPs work better when the size is smaller than the critical value, i.e. 10–20 nm [68]. Effectively controlled at such a low scale, the magnetic properties of NPs make these particles priceless and can be used in different applications [31, 68, 69]. In NPs, the uneven electronic distribution causes the magnetic property development [70, 71].

1.5.3 Mechanical Properties

Researchers can find new applications in a wide range of necessary sectors, including tribology, surface engineering, and nano-making, thanks to its distinct mechanical properties. A mechanical study of the automated nature of the NPs involves elastic modulus, hardness, stress, vibration, adhesion, and friction. Coagulation and lubrication also help improve the mechanical characteristics of the NPs and this parameter [72]. NPs exhibit different mechanical properties in contrast with microparticles and their bulk materials. Furthermore, comparing the steepness between NPs and the external contact surface checking on a lubricated or grated contact reveals that the NPs operate in a communication setup. Decent checks and interactions between the NPs' mechanical characteristics and any surface shape are critical for improving surface quality and enhancing material elimination. In these areas, a strong understanding of the fundamental mechanical aspects of NPs, including the elastic module and the hardness, motion, friction, and input, typically requires good performance [72].

1.5.4 Thermal Properties

The thermal conductivity of NP metals is known to be higher than that of stable fluids. For example, the thermal copper conductivity is about 700 times higher than water and approximately 3000 times higher than engine oil at room temperature. In addition, alumina oxides (Al_2O_3) are thermally more thermally capable than water. Fluids containing solids suspended with higher thermal conductance should therefore be substantially higher than conventional heat transmission fluid. Dispersing the nanometric scales solid particles into liquid such as water, ethylene glycol or oils produces nanofluids. Dispersed nanometric scale nanofluids are supposed to exhibit superior propensities compared to conventional heat transfer fluids and fluids containing microscopic particles. As this thermal transfer occurs on the particles' surface, it is essential to use particles with a large overall surface region. The wider total area also improves the stability of the suspension [73]. It has recently been shown that advanced thermal conductivity is exhibited by nanofluids consisting of CuO or Al_2O_3 NPs in water or ethylene [74].

1.6 Functions of NPs

The NPs find their application in almost every day-to-day utility, and some of the significant applications are discussed as follows:

1.6.1 Drugs and Medications

The basic physical and chemical properties of single or multiple nano-sized inorganic particles are becoming an increasingly valuable commodity in developing novel nanoequipment used in many different physical, biological, biomedical, and therapeutic products [75].

Throughout every medicine market, the importance of NPs in delivering drugs in the best dosage range has improved. This has sometimes resulted in an improvement in the medicines' clinical efficiency, weakened side effects, and improved patient compliance [76]. Iron oxide particles such as magnetite (Fe_3O_4) or its oxidized form of maghemite (Fe_2O_3) are most widely used for biomedical applications [77]. For biological and cell imaging applications and photothermal therapeutic applications, the option of NPs to achieve efficient contrast is based on the optical properties of NPs [78]. Over the past few years, hydrophilic NP development as a drug carrier has represented a significant challenge. Polyethylene oxide (PEO) and polylactic acid (PLA) NPs were established as an excellent method for intravenous drug administration among the different approaches [79]. For various in vivo applications, such as MRI contrast enhancement, tissue repair and immunoassay, detoxification of biological fluids, hyperthermia, drug delivery, and cell separation, superparamagnetic iron oxide NPs with good surface chemistry can be used [80]. Antibodies labelled with fluorescent dyes, enzymes, radioactive compounds, or colloidal Au [67] can be used to detect analytes in tissue parts via antigen–antibody interactions.

The specific benefits of liposomes, including the capability to shield drugs from degradation, target them at their active sites, and minimize harmfulness and other side effects, are a possible carrier instead of traditional dosage types. The polymeric NPs provide some significant advantages over the liposomes of these materials. NPs, for example, help improve drug ratability and provide convenient, controlled drug release properties. The extreme absorbed light is effectively converted into localized heat by Au-NPs, which can be used for targeted laser photothermal cancer therapy [81, 82]. Besides this, to prevent tumour development, the antineoplastic effect of NPs is also effectively used. Compared to organic compounds that are comparatively toxic to biological systems, the antimicrobial properties of inorganic NPs add more potency to this essential feature [83–85]. To selectively overcome the microbial cells, the NPs are engaged with various classes. Because of their adequate antibacterial efficacy, TiO_2, ZnO, $BiVO_4$, and Cu- and Ni-based NPs have been used for this reason [86].

1.6.2 Materials and Manufacturing

The NP manufacturer displays physicochemical characteristics that induce specific electrical, mechanical, optical, and imaging properties that are highly sought for applications in the medical, commercial, and ecological sectors in particular [87]. NPs focus on biological and non-biological characterization, design, and engineering of <100 nm structures, exhibiting new and unique characteristics. Many producers at high and low levels have reported the potential benefits of nanotechnology. Mass production of marketable products such as microelectronics, aerospace, and pharmaceutical companies are now underway [88]. Many industries have indicated that nanotechnology is the next development, including food processing and packaging. RET (organic dye molecules and noble metals) has been considered in the recent interest in biophotonics and materials science [89]. The plasmon

resonance arising from the reciprocal oscillation of electrons at the surface of the NP [89, 90] is distinctly coloured in NP metals, such as noble metals, such as Au and Ag.

1.6.3 Environment

The release of these materials to the atmosphere contributes to commercial and domestic engineered nuclear power plants [91]. The use of engineering materials would increase soil and groundwater NP concentrations, which provide the most significant exposure pathways for assessing environmental risk [92]. During the formation of natural NPs, the surface of NPs can be consumed, co-precipitated, or stuck with the accumulation of NPs containing toxins adsorbed to their bodies by a vast specific-to-mass proportion of natural NPs. NP pollutants' interaction depends on the characteristics of NPs, such as scale, composition, morphology, porosity and aggregation, and structure [93]. The following attributes of NPs make the ideal theme candidate for environmentally friendly goods, sanitation of toxic substance-contaminated materials, and ecological stage sensors [10]. Superparamagnetic iron oxide NPs are a valuable sorbent material for this harmful soft material [94, 95].

NP photodegradation is also a generalized method, which includes the use of several nanomaterials. For photodegradation, Rogozea et al. revealed in a tandem fashion that modified silica NiO/ZnO has been productive because of the minimum size of the high NP surface (<10 nm) [96].

1.6.4 Electronics

In recent years, there has been rising interest in printed electronics production because printed electronics offer the potential for low-cost, large-area electronics for flexible displays and sensors appealing to conventional silicon techniques. As a mass manufacturing process for new forms of electronic equipment, printed electronics with various functional inks containing NPs such as metallic NPs, organic electronic molecules, CNTs, and ceramic NPs are expected to flow quickly [97, 98]. An excellent example of the synergies between scientific discovery and technological growth is the electronic industry. The findings of new semiconducting materials have led to a revolution from aspirated tubes to diodes and transistors and finally to miniature chips [10, 99]. The critical characteristics of NPs that make nanotechnology benchmarks [100] possible for NP to be used in electrical, electronic, or optical applications, including bottom-up or self-assembly frameworks, are easy handling.

1.6.5 Energy Harvesting

Because of their large surface area, optical behaviour, and catalytic nature, scientists are changing their research strategies to produce renewable energies from readily available resources at low cost. NPs are the best candidate for this reason. NPs are widely used to generate power from photoelectrochemical (PEC) and electrochemical water splitting [48], especially in photocatalytic applications. Electrochemical CO_2 reduction in fuel precursors, solar cells, and piezoelectric generators also provided advanced energy generation options in addition to water splitting [34]. NPs are often used in energy storage applications to reserve animations in various ways at the nanoscale level [101, 102]. Nanogenerators have

recently been developed to transform mechanical energy into electricity using piezoelectric power, an unconventional approach to power generation [103].

References

1 Feynman, R.P. (1960). There's plenty of room at the bottom. *Eng. Sci.* 22: 22–36.
2 Khan, I., Saeed, K., and Khan, I. (2017). Nanoparticles: properties, applications and toxicities. *Arabian J. Chem.* 12: 908–931.
3 Tiwari, J.N., Tiwari, R.N., and Kim, K.S. (2012). Zero-dimensional, one-dimensional, two-dimensional and three-dimensional nanostructured materials for advanced electrochemical energy devices. *Prog. Mater. Sci.* 57: 724–803. https://doi.org/10.1016/j.pmatsci.2011.08.003.
4 Dreaden, E.C., Alkilany, A.M., Huang, X. et al. (2012). The golden age: gold nanoparticles for biomedicine. *Chem. Soc. Rev.* 41: 2740–2779. https://doi.org/10.1039/C1CS15237H.
5 Shin, W.K., Cho, J., Kannan, A.G. et al. (2016). Cross-linked composite gel polymer electrolyte using mesoporous methacrylate-functionalized SiO_2 nanoparticles for lithium-ion polymer batteries. *Sci. Rep.* 6: 26332. https://doi.org/10.1038/srep26332.
6 Lee, J.E., Lee, N., Kim, T. et al. (2011). Multifunctional mesoporous silica nanocomposite nanoparticles for theranostic applications. *Acc. Chem. Res.* 44: 893–902. https://doi.org/10.1021/ar2000259.
7 Barrak, H., Saied, T., Chevallier, P. et al. (2016). Synthesis, characterization, and functionalization of ZnO nanoparticles by *N*-(trimethoxysilylpropyl) ethylenediamine tri acetic acid (TMSEDTA): an investigation of the interactions between phloroglucinol and ZnO@TMSEDTA. *Arabian J. Chem.* https://doi.org/10.1016/j.arabjc.2016.04.019.
8 Ullah, H., Khan, I., Yamani, Z.H., and Qurashi, A. (2017). Sonochemical-driven ultrafast facile synthesis of SnO_2 nanoparticles: growth mechanism structural electrical and hydrogen gas sensing properties. *Ultrason. Sonochem.* 34: 484–490. https://doi.org/10.1016/j.ultsonch.2016.06.025.
9 Ramacharyulu, P.V.R.K., Muhammad, R., Praveen Kumar, J. et al. (2015). Iron phthalocyanine modified mesoporous titania nanoparticles for photocatalytic activity and CO_2 capture applications. *Phys. Chem. Chem. Phys.* 17: 26456–26462. https://doi.org/10.1039/C5CP03576G.
10 Shaalan, M., Saleh, M., El-Mahdy, M., and El-Matbouli, M. (2016). Recent progress in applications of nanoparticles in fish medicine: a review. *Nanomed. Nanotechnol. Biol. Med.* 12: 701–710. https://doi.org/10.1016/j.nano.2015.11.005.
11 Astefanei, A., Núñez, O., and Galceran, M.T. (2015). Characterization and determination of fullerenes: a critical review. *Anal. Chim. Acta* 882: 1–21. https://doi.org/10.1016/j.aca.2015.03.025.
12 Ibrahim, K.S. (2013). Carbon nanotubes-properties and applications: a review. *Carbon Lett.* 14: 131–144. https://doi.org/10.5714/CL.2013.14.3.131.
13 Aqel, A., El-Nour, K.M.M.A., Ammar, R.A.A., and Al-Warthan, A. (2012). Carbon nanotubes, science and technology part (I) structure, synthesis and characterization. *Arabian J. Chem.* 5: 1–23. https://doi.org/10.1016/j.arabjc.2010.08.022.

14 Elliott, J.A., Shibuta, Y., Amara, H. et al. (2013). Atomistic modelling of CVD synthesis of carbon nanotubes and graphene. *Nanoscale* 5: 6662. https://doi.org/10.1039/c3nr01925j.

15 Saeed, K. and Khan, I. (2016). Preparation and characterization of single-walled carbon nanotube/nylon 6,6 nanocomposites. *Instrum Sci. Technol.* 44: 435–444. https://doi.org/10.1080/10739149.2015.1127256.

16 Ngoy, J.M., Wagner, N., Riboldi, L., and Bolland, O. (2014). A CO_2 capture technology using multi-walled carbon nanotubes with polyaspartamide surfactant. *Energy Procedia* 63: 2230–2248. https://doi.org/10.1016/j.egypro.2014.11.242.

17 Mabena, L.F., Sinha Ray, S., Mhlanga, S.D., and Coville, N.J. (2011). Nitrogen-doped carbon nanotubes as a metal catalyst support. *Appl. Nanosci.* 1: 67–77. https://doi.org/10.1007/s13204-011-0013-4.

18 Sigmund, W., Yuh, J., Park, H. et al. (2006). Processing and structure relationships in electrospinning of ceramic fiber systems. *J. Am. Ceram. Soc.* 89: 395–407. https://doi.org/10.1111/j.1551-2916.2005.00807.x.

19 Thomas, S., Harshita, B.S.P., Mishra, P., and Talegaonkar, S. (2015). Ceramic nanoparticles: fabrication methods and applications in drug delivery. *Curr. Pharm. Des.* 21: 6165–6188. https://doi.org/10.2174/1381612821666151027153246.

20 Ali, S., Khan, I., Khan, S.A. et al. (2017). Electrocatalytic performance of Ni@Pt core-shell nanoparticles supported on carbon nanotubes for methanol oxidation reaction. *J. Electroanal. Chem.* 795: 17–25. https://doi.org/10.1016/j.jelechem.2017.04.040.

21 Sun, S. (2000). Monodisperse FePt nanoparticles and ferromagnetic FePt nanocrystal superlattices. *Science* 80 (287): 1989–1992. https://doi.org/10.1126/science.287.5460.1989.

22 Hisatomi, T., Kubota, J., and Domen, K. (2014). Recent advances in semiconductors for photocatalytic and photoelectrochemical water splitting. *Chem. Soc. Rev.* 43: 7520–7535. https://doi.org/10.1039/C3CS60378D.

23 Abouelmagd, S.A., Meng, F., Kim, B.-K. et al. (2016). Tannic acid-mediated surface functionalization of polymeric nanoparticles. *ACS Biomater. Sci. Eng.*: 6b00497. https://doi.org/10.1021/acsbiomaterials.6b004.

24 Rawat, M.K., Jain, A., Singh, S. et al. (2011). Studies on binary lipid matrix-based solid lipid nanoparticles of repaglinide: in vitro and in vivo evaluation. *J. Pharm. Sci.* 100: 2366–2378. https://doi.org/10.1002/jps.22435.

25 Mashaghi, S., Jadidi, T., Koenderink, G., and Mashaghi, A. (2013). Lipid nanotechnology. *Int. J. Mol. Sci.* 14: 4242–4282. https://doi.org/10.3390/ijms14024242.

26 Puri, A., Loomis, K., Smith, B. et al. (2009). Lipid-based nanoparticles as pharmaceutical drug carriers: from concepts to clinic. *Crit. Rev. Ther. Drug Carrier Syst.* 26: 523–580.

27 Gujrati, M., Malamas, A., Shin, T. et al. (2014). Multifunctional cationic lipid-based nanoparticles facilitate endosomal escape and reduction-triggered cytosolic siRNA release. *Mol. Pharmaceutics* 11: 2734–2744. https://doi.org/10.1021/mp400787s.

28 Wang, Y. and Xia, Y. (2004). Bottom-up and top-down approaches to the synthesis of monodispersed spherical colloids of low melting-point metals. *Nano Lett.* 4: 2047–2050. https://doi.org/10.1021/nl048689j.

29 Iravani, S. (2011). Green synthesis of metal nanoparticles using plants. *Green Chem.* 13: 2638. https://doi.org/10.1039/c1gc15386b.

30 Bello, S.A., Agunsoye, J.O., and Hassan, S.B. (2015). Synthesis of coconut shell nanoparticles via a top-down approach: assessment of milling duration on the particle sizes and morphologies of coconut shell nanoparticles. *Mater. Lett.* https://doi.org/10.1016/j.matlet.2015.07.063.

31 Priyadarshana, G., Kottegoda, N., Senaratne, A. et al. (2015). Synthesis of magnetite nanoparticles by top-down approach from a high purity ore. *J. Nanomater.*: 1–8. https://doi.org/10.1155/2015/317312.

32 Garrigue, P., Delville, M.-H., Labruge're, C. et al. (2004). Top-down approach for the preparation of colloidal carbon nanoparticles. *Chem. Mater.* 16: 2984–2986. https://doi.org/10.1021/cm049685i.

33 Zhang, X., Lai, Z., Liu, Z. et al. (2015). A facile and universal top-down method for preparation of monodisperse transition-metal dichalcogenide nanodots. *Angew. Chem. Int. Ed.* 54: 5425–5428. https://doi.org/10.1002/anie.201501071.

34 Zhou, Y., Dong, C.K., Han, L. et al. (2016). Top-down preparation of active cobalt oxide catalyst. *ACS Catal.* 6: 6699–6703. https://doi.org/10.1021/acscatal.6b02416.

35 Mogilevsky, G., Hartman, O., Emmons, E.D. et al. (2014). Bottom-up synthesis of anatase nanoparticles with graphene domains. *ACS Appl. Mater. Interfaces* 6: 10638–10648. https://doi.org/10.1021/am502322y.

36 Liu, D., Li, C., Zhou, F. et al. (2015). Rapid synthesis of monodisperse Au nanospheres through a laser irradiation-induced shape conversion, self-assembly and their electromagnetic coupling SERS enhancement. *Sci. Rep.* 5: 7686. https://doi.org/10.1038/srep07686.

37 Liu, J., Liu, Y., Liu, N. et al. (2015). Metal-free efficient photocatalyst for stable visible water splitting via a two-electron pathway. *Science* 80 (347): 970–974. https://doi.org/10.1126/science.aaa3145.

38 Needham, D., Arslanagic, A., Glud, K. et al. (2016). Bottom-up design of nanoparticles for anti-cancer diapeutics: "put the drug in the cancer's food". *J. Drug Targeting*: 1–21. https://doi.org/10.1080/1061186X.2016.1238092.

39 Wang, Y. and Xia, Y. (2004). Bottom-up and top-down approaches to synthesizing monodispersed spherical colloids of low melting-point metals. *Nano Lett.* 4: 2047–2050. https://doi.org/10.1021/nl048689j.

40 Parveen, K., Banse, V., and Ledwani, L. (2016). Green synthesis of nanoparticles: their advantages and disadvantages. *Acta Naturae*: 20048. https://doi.org/10.1063/1.4945168.

41 Ahmed, S., Annu, S., and Yudha, S.S. (2016). Biosynthesis of gold nanoparticles: a green approach. *J. Photochem. Photobiol., B* 161: 141–153. https://doi.org/10.1016/j.jphotobiol.2016.04.034.

42 Biswas, A., Bayer, I.S., Biris, A.S. et al. (2012). Advances in top-down and bottom-up surface nanofabrication: techniques, applications and prospects. *Adv. Colloid Interface Sci.* 170: 2–27. https://doi.org/10.1016/j.cis.2011.11.001.

43 Mirzadeh, E. and Akhbari, K. (2016). Synthesis of nanomaterials with desirable morphologies from metal–organic frameworks for various applications. *CrystEngComm* 18: 7410–7424. https://doi.org/10.1039/C6CE01076H.

44 Khlebtsov, N. and Dykman, L. (2011). Biodistribution and toxicity of engineered gold nanoparticles: a review of in vitro and in vivo studies. *Chem. Soc. Rev.* 40: 1647–1671. https://doi.org/10.1039/C0CS00018C.

45 Wang, J., Yang, N., Tang, H. et al. (2013). Accurate control of multishelled Co_3O_4 hollow microspheres as high-performance anode materials in lithium-ion batteries. *Angew. Chem. Int. Ed.* 52: 6417–6420. https://doi.org/10.1002/anie.201301622.

46 Emery, A.A., Saal, J.E., Kirklin, S. et al. (2016). High-throughput computational screening of perovskites for thermochemical water splitting applications. *Chem. Mater.* 28 https://doi.org/10.1021/acs.chemmater.6b01182.

47 Ingham, B. (2015). X-ray scattering characterization of nanoparticles. *Crystallogr. Rev.* 21: 229–303. https://doi.org/10.1080/0889311X.2015.1024114.

48 Avasare, V., Zhang, Z., Avasare, D. et al. (2015). Room-temperature synthesis of TiO_2 nanospheres and their solar-driven photoelectrochemical hydrogen production. *Int. J. Energy Res.* 39: 1714–1719. https://doi.org/10.1002/er.3372.

49 Khan, I., Ali, S., Mansha, M., and Qurashi, A. (2017). Sonochemical assisted hydrothermal synthesis of pseudo-flower shaped Bismuth vanadate ($BiVO_4$) and their solar-driven water splitting application. *Ultrason. Sonochem.* 36: 386–392. https://doi.org/10.1016/j.ultsonch.2016.12.014.

50 Mansha, M., Qurashi, A., Ullah, N. et al. (2016). Synthesis of In_2O_3/graphene heterostructure and their hydrogen gas sensing properties. *Ceram. Int.* 42: 11490–11495. https://doi.org/10.1016/j.ceramint.2016.04.035.

51 Lykhach, Y., Kozlov, S.M., Skála, T. et al. (2015). Counting electrons on supported nanoparticles. *Nat. Mater.* https://doi.org/10.1038/nmat4500.

52 Oprea, B., Martínez, L., Román, E. et al. (2015). Dispersion and functionalization of nanoparticles synthesized by gas aggregation source: opening new routes toward the fabrication of nanoparticles for biomedicine. *Langmuir* 31: 13813–13820. https://doi.org/10.1021/acs.langmuir.5b03399.

53 Wang, Y.C., Engelhard, M.H., Baer, D.R., and Castner, D.G. (2016). Quantifying the impact of nanoparticle coatings and nonuniformities on XPS analysis: gold/silver core-shell nanoparticles. *Anal. Chem.* 88: 3917–3925. https://doi.org/10.1021/acs.analchem.6b00100.

54 Dablemont, C., Lang, P., Mangeney, C. et al. (2008). FTIR and XPS study of Pt nanoparticle functionalization and interaction with alumina. *Langmuir* 24: 5832–5841. https://doi.org/10.1021/la7028643.

55 Pokhrel, M., Wahid, K., and Mao, Y. (2016). Systematic studies on RE_2-Hf_2O_7:5%Eu^{3+} (RE = Y, La, Pr, Gd, Er, and Lu) nanoparticles: effects of the A-site RE^{3+} cation and calcination on structure and photoluminescence. *J. Phys. Chem. C* 120: 14828–14839. https://doi.org/10.1021/acs.jpcc.6b04798.

56 Muehlethaler, C., Leona, M., and Lombardi, J.R. (2016). Review of surface-enhanced Raman scattering applications in forensic science. *Anal. Chem.* 88: 152–169. https://doi.org/10.1021/acs.analchem.5b04131.

57 Ma, S., Livingstone, R., Zhao, B., and Lombardi, J.R. (2011). Enhanced Raman spectroscopy of nanostructured semiconductor phonon modes. *J. Phys. Chem. Lett.* 2: 671–674. https://doi.org/10.1021/jz2001562.

58 Sikora, A., Shard, A.G., and Minelli, C. (2016). Size and ζ-potential measurement of silica nanoparticles in serum using tunable resistive pulse sensing. *Langmuir* 32: 2216–2224. https://doi.org/10.1021/acs.Langmuir.5b04160.

59 Filipe, V., Hawe, A., and Jiskoot, W. (2010). Critical evaluation of nanoparticle tracking analysis (NTA) by insight to measure nanoparticles and protein aggregates. *Pharm. Res.* 27: 796–810. https://doi.org/10.1007/s11095-010-0073-2.

60 Gross, J., Sayle, S., Karow, A.R. et al. (2016). Nanoparticle tracking analysis of particle size and concentration detection in suspensions of polymer and protein samples: influence of experimental and data evaluation parameters. *Eur. J. Pharm. Biopharm.* 104: 30–41. https://doi.org/10.1016/j.ejpb.2016.04.013.

61 Cho, C.H., Aspetti, C.O., Park, J., and Agarwal, R. (2013). Silicon coupled with plasmon nanocavities generates bright visible hot luminescence. *Nat. Photonics* 7: 285–289.

62 Chowdhury, F.I., Nayfeh, M.H., and Nayfeh, A.M. (2016). Enhanced performance of thin-film silicon solar cells with a top film of silicon nanoparticles due to down-conversion and near resonance charge transport. *J. Sol. Energy* 125: 332–338.

63 Swinehart, D.F. (1962). The Beer-Lambert law. *J. Chem. Educ.* 39: 333. https://doi.org/10.1021/ed039p333.

64 Peng, K., Fu, L., Yang, H., and Ouyang, J. (2016). Perovskite $LaFeO_3$/−montmorillonite nanocomposites: synthesis, interface characteristics and enhanced photocatalytic activity. *Sci. Rep.* 6: 19723. https://doi.org/10.1038/srep19723.

65 Eustis, S. and El-Sayed, M.A. (2006). Why gold nanoparticles are more precious than pretty gold: noble metal surface plasmon resonance and enhancement of the radiative and nonradiative properties of nanocrystals of different shapes. *Chem. Soc. Rev.* 35: 209–217. https://doi.org/10.1039/B514191E.

66 Khlebtsov, N. and Dykman, L. (2010). Optical properties andbiomedical applications of plasmonic nanoparticles. *J. Quant. Spectrosc. Radiat. Transf.* 111: 1–35. https://doi.org/10.1016/j.jqsrt.2009.07.012.

67 Khlebtsov, N.G. and Dykman, L.A. (2010). Optical properties and biomedical applications of plasmonic nanoparticles. *J. Quant. Spectrosc. Radiat. Transfer* 111: 1–35. https://doi.org/10.1016/j.jqsrt.2009.07.012.

68 Reiss, G. and Hutten, A. (2005). Magnetic nanoparticles: applications beyond data storage. *Nat. Mater.* 4: 725–726. https://doi.org/10.1038/nmat1494.

69 Faivre, D. and Bennet, M. (2016). Materials science: magnetic nanoparticles line up. *Nature* 535: 235–236. https://doi.org/10.1038/535235a.

70 Qi, M., Zhang, K., Li, S. et al. (2016). Superparamagnetic Fe_3O_4 nanoparticles: synthesis by a solvothermal process and functionalization for a magnetic targeted curcumin delivery system. *New J. Chem.* 4480: 4480–4491. https://doi.org/10.1039/c5nj02441b.

71 Wu, W., He, Q., and Jiang, C. (2008). Magnetic iron oxide nanoparticles: synthesis and surface functionalization strategies. *Nanoscale Res. Lett.* 3: 397–415. https://doi.org/10.1007/s11671-008-9174-9.

72 Guo, D., Xie, G., and Luo, J. (2014). Mechanical properties of nanoparticles: basics and applications. *J. Phys. D: Appl. Phys.* 47: 13001. https://doi.org/10.1088/0022-3727/47/1/013001.

73 Lee, S., Choi, S.U.-S., Li, S., and Eastman, J.A. (1999). Measuring thermal conductivity of fluids containing oxide nanoparticles. *J. Heat Transfer* 121: 280–285. https://doi.org/10.1115/1.2825978.

74 Cao, Y.C. (2002). Nanoparticles with Raman spectroscopic fingerprints for DNA and RNA detection. *Science* 80 (297): 1536–1540. https://doi.org/10.1126/science.297.5586.1536.

75 Loureiro, A., Azoia, N.G., Gomes, A.C., and Cavaco-Paulo, A. (2016). Albumin-based nanodevices as drug carriers. *Curr. Pharm. Des.* 22: 1371–1390.

76 Alexis, F., Pridgen, E., Molnar, L.K., and Farokhzad, O.C. (2008). Factors affecting the clearance and biodistribution of polymeric nanoparticles. *Mol. Pharmaceutics* 5: 505–515. https://doi.org/10.1021/mp800051m.

77 Ali, A., Zafar, H., Zia, M. et al. (2016). Synthesis, characterization, applications, and challenges of iron oxide nanoparticles. *Nanotechnol. Sci. Appl* 9: 49–67. https://doi.org/10.2147/NSA.S99986.

78 Jain, P.K., Lee, K.S., El-Sayed, I.H., and El-Sayed, M.A. (2006). Calculated absorption and scattering properties of gold nanoparticles different size, shape, and composition: applications in biological imaging and biomedicine. *J. Phys. Chem. B* 110: 7238–7248. https://doi.org/10.1021/jp057170o.

79 Calvo, P., Remuoon-Lopez, C., Vila-Jato, J.L., and Alonso, M.J. (1997). Novel hydrophilic chitosan-polyethylene oxide nanoparticles as protein carriers. *J. Appl. Polym. Sci.* 63: 125–132. https://doi.org/10.1002/(SICI)1097-4628(19970103)63:1*125::AID-APP13*3.0.CO;2-4.

80 Laurent, S., Forge, D., Port, M. et al. (2010). Magnetic iron oxide nanoparticles: synthesis, stabilization, vectorization, physicochemical characterizations, and biological applications. *Chem. Rev.* 110: 2064–2110. https://doi.org/10.1021/cr900197g.

81 Zhang, J. and Saltzman, M. (2013). Engineering biodegradable nanoparticles for drug and gene delivery. *Chem. Eng. Prog.* 109: 25–30.

82 Prashant, K.J. and Ivan, H.S. (2007). Au NPs target cancer. *Nano Today* 2: 19–29.

83 Chen, C., Xing, G., Wang, J. et al. (2005). Multihydroxylated $[Gd@C_{82}(OH)_{22}]_n$ nanoparticles: antineoplastic activity of high efficiency and low toxicity. *Nano Lett.* 5: 2050–2057. https://doi.org/10.1021/nl051624b.

84 AshaRani, P.V., Low Kah Mun, G., Hande, M.P., and Valiyaveettil, S. (2009). Cytotoxicity and genotoxicity of silver nanoparticles in human cells. *ACS Nano* 3: 279–290. https://doi.org/10.1021/nn800596w.

85 Hajipour, M.J., Fromm, K.M., Ashkarran, A.A. et al. (2012). Antibacterial properties of nanoparticles. *Trends Biotechnol.* 30: 499–511. https://doi.org/10.1016/j.tibtech.2012.06.004.

86 Yin, Q., Wu, W., Qiao, R. et al. (2016). Glucose assisted transformation of Ni-doped-ZnO@carbon to a Ni-dopedZnO@void@SiO_2 core–shell nanocomposite photocatalyst. *RSC Adv.* 6: 38653–38661. https://doi.org/10.1039/C5RA26631A.

87 Todescato, F., Fortunati, I., Minotto, A. et al. (2016). Engineering of semiconductor nanocrystals for light-emitting applications. *Materials* 9: 672. https://doi.org/10.3390/ma9080672.

88 Weiss, J., Takhistov, P., and McClements, D.J. (2006). Functional materials in food nanotechnology. *J. Food Sci.* 71: R107–R116. https://doi.org/10.1111/j.1750-3841.2006.00195.x.

89 Lei, Y.-M., Huang, W.-X., Zhao, M. et al. (2015). Electrochemiluminescence resonance energy transfer system: mechanism and application in ratiometric aptasensor for lead ion. *Anal. Chem.* 87: 7787–7794. https://doi.org/10.1021/acs.analchem.5b01445.

90 Unser, S., Bruzas, I., He, J., and Sagle, L. (2015). Localized surface plasmon resonance biosensing: current challenges and approaches. *Sensors* 15: 15684–15716. https://doi.org/10.3390/s150715684.

91 Ripp, S. and Henry, T.B. (eds.) (2011). *Biotechnology and Nanotechnology Risk Assessment: Minding and Managing the Potential Threats Around Us*, ACS Symposium Series. Washington, DC: American Chemical Society http://dx.doi.org/10.1021/bk-2011-1079.

92 Golobič, M., Jemec, A., Drobne, D. et al. (2012). Upon exposure to Cu nanoparticles, accumulation of copper in the isopod *Porcellio scaber* is due to the dissolved Cu ions inside the digestive tract. *Environ. Sci. Technol.* 46: 12112–12119. https://doi.org/10.1021/es3022182.

93 Swadeshmukul, S., Peng, Z., Kemin, W. et al. (2001). Conjugation of biomolecules with luminophore-doped silica nanoparticles for photostable biomarkers. *Anal. Chem.* 73: 4988–4993. https://doi.org/10.1021/AC010406+.

94 Tratnyek, P.G. and Johnson, R.L. (2006). Nanotechnologies for environmental cleanup. *Nano Today* 1: 44–48. https://doi.org/10.1016/S1748-0132(06)70048-2.

95 Mueller, N.C. and Nowack, B. (2008). Exposure modeling of engineered nanoparticles in the environment. *Environ. Sci. Technol.* 42: 4447–4453. https://doi.org/10.1021/es7029637.

96 Rogozea, E.A., Petcu, A.R., Olteanu, N.L. et al. (2017). Tandem adsorption-photodegradation activity induced by light on NiO-ZnO *p–n* couple modified silica nanomaterials. *Mater. Sci. Semicond. Process.* 57: 1–11. https://doi.org/10.1016/j.mssp.2016.10.006.

97 Rogozea, E.A., Olteanu, N.L., Petcu, A.R. et al. (2016). Extension of optical properties of ZnO/SiO_2 materials induced by incorporation of Au or NiO nanoparticles. *Opt. Mater.* 56: 45–48. https://doi.org/10.1016/j.optmat.2015.12.020.

98 Kosmala, A., Wright, R., Zhang, Q., and Kirby, P. (2011). Synthesis of silver nanoparticles and fabrication of aqueous Ag inks for inkjet printing. *Mater. Chem. Phys.* 129: 1075–1080. https://doi.org/10.1016/j.matchemphys.2011.05.064.

99 Cushing, B.L., Kolesnichenko, V.L., and O'Connor, C.J. (2004). Recent advances in the liquid-phase syntheses of inorganic nanoparticles. *Chem. Rev.* 104: 3893–3946. https://doi.org/10.1021/cr030027b.

100 O'Brien, S., Brus, L., and Murray, C.B. (2001). Synthesis of monodisperse nanoparticles of barium titanate: toward a generalized oxide nanoparticle synthesis strategy. *J. Am. Chem. Soc.* 123: 12085–12086. https://doi.org/10.1021/ja011414a.

101 Wang, D.W. and Su, D. (2014). Heterogeneous nanocarbon materials for the oxygen reduction reaction. *Energy Environ. Sci.* 7: 576. https://doi.org/10.1039/c3ee43463j.

102 Wang, Z., Pan, X., He, Y. et al. (2015). Piezoelectric nanowires in energy harvesting applications. *Adv. Mater. Sci. Eng.* 2015: 1–21. https://doi.org/10.1155/2015/165631.

103 Kot, M., Major, Ł., Lackner, J.M. et al. (2016). Mechanical and tribological properties of carbon-based graded coatings. *J. Nanomater.* 2016: 1–14. https://doi.org/10.1155/2016/8306345.